Influence of Spray Parameters on the Features of Gas Tunnel Type Plasma Sprayed Hydroxyapatite Coatings†

MORKS F. Magdi* and KOBAYASHI Akira**

Abstract

Hydroxyapatite coatings were deposited on 304 stainless steel substrates by using the gas tunnel type plasma spraying process. The influences of spraying distances and arc currents on the microstructure, adhesion and hardness properties of HA coatings were investigated. The results showed that HA coatings sprayed at low power have a porous structure and poor hardness. HA coatings sprayed at high power and short spraying distance are characterized by good adhesion and low porosity with dense structure. The hardness of the HA coatings sprayed at short spraying distance and higher plasma power was increased, mainly due to the formation of dense coatings.

KEYWORDS: (Hydroxyapatite), (Gas tunnel type plasma spraying), (Spraying distances), (Plasma power), (Microstructure), (Adhesion), (Hardness)

1. Introduction

Although metallic implants such as Ti, Ti-alloys and stainless steel show good mechanical properties for use in biomedical applications they exhibit low biocompatibility with body fluids. Surface modification is required for the metallic implants to improve their biocompatibility properties. Hydroxyapatite is extensively used for surface improvement of the metallic implants because it exhibits good compatibility with body fluids[1-3]. Many methods have been used to deposit HA coatings on implant surfaces such as conventional press-and-sinter methods, ion beam sputtering, electrophoretic deposition, R.F.-magnetron sputtering, pulse laser melting, physical vapor deposition and electrochemical deposition[4-10]. Thermal spraying processes (e.g. plasma and HVOF) are the fastest methods for depositing thick and dense HA coatings with good adhesion with the substrate[11-13]. Conventional plasma spraying is used for this purpose and some studies[14, 15] have been done to optimize the spray parameters to get high quality HA coatings.

Gas tunnel type plasma spraying is a high power plasma system[16-19] and has the ability to deposit a thick HA coatings (> 500 μm) with good adhesion with the substrate [20]. In this study we used this system to deposit high crystalline HA coatings at different spray distances and arc currents. Microstructure and mechanical properties such as hardness of the resulting HA coatings were investigated.

2. Experimental Procedure

2.1 Materials

Commercial HA powders of particle size 10 – 45 μm were used as spray materials. The spherical starting powders are highly crystallized pure HA phase as shown by the X-ray diffraction pattern in **Fig. 1**. The powders were sprayed on 304 stainless steel substrates of dimensions 30X30X2.5 mm. Prior to spraying, the substrate surface was grit blasted with alumina to roughen and clean the surface and followed by cleaning using acetone.

2.2. Plasma spraying

HA powders were atmospherically plasma sprayed (APS) using the gas tunnel type plasma process at different spray distances and arc currents. The spray conditions used in this investigation is listed in **Table 1**. Argon was used as both the primary and the carrier gas. The powders were externally fed into the plasma flame. The substrates were initially pre-heated by plasma flame at around 600 K. For studying the effect of spray distances, the arc current was kept constant at 500 A for all experiments done at different spray distances.

2.3 Characterization techniques

The microstructure of feedstock and coatings were observed using ERA8800FE scanning electron microscope. The examined cross-section samples were mounted in epoxy resin, polished and buffed with alumina paste (1.0, 0.3, and 0.05 μm, respectively) to get a mirror finished surface. All examined samples were coated with a thin film of gold using a gold ion sputtering system to make them electrically conductive before SEM observation.

Phase identification of feedstock and HA coatings was carried out using JEOL JDX-3530M X-ray diffractometer system with CuKα radiation source; the operating voltage was 40 kV and current 40 mA.

† Received on November.7, 2005
* Foreign Visiting Researcher
** Associate Professor
Transactions of JWRI is published by Joining and Welding Research Institute, Osaka University, Ibaraki, Osaka 567-0047, Japan

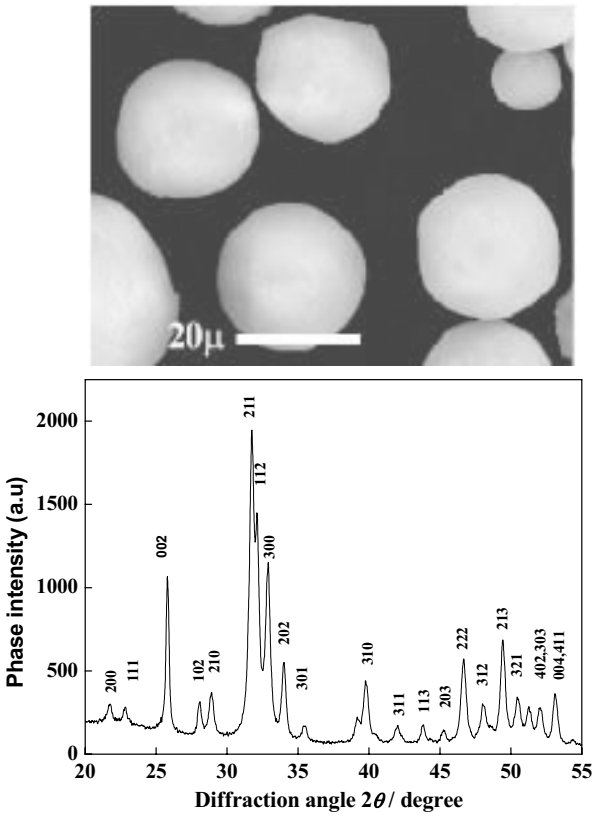

Fig. 1 SEM micrograph and X-ray diffraction pattern of the starting HA powder.

Table 1 Spraying conditions of HA powders used in this paper.

Powder Type	Hydroxyapatite Powder
Particle Size, μm	$10 > dp > 45$
Primary gas flow rate (Ar), l/min	120
Carrier gas flow rate, l/min	7
Powder flow rate, g/min	20
Arc current, A	250, 300, 350, 400, 450, 500
Spraying distances, mm	60, 70, 80, 90

Hardness tests were performed on polished and buffed cross-section coated samples using AKASHI AAV-500 series hardness tester. The load used was 490.3 mN and the load time was 20 s. Each hardness value is the average of 7 readings.

Porosity of HA coatings was evaluated by the image analyzing method using a computerized optical microscope.

3. Results and Discussions

3.1 Phase structure of HA coatings sprayed at different spraying distances and arc currents

X-ray diffraction patterns of HA coatings sprayed at different spraying distances and arc currents are shown in **Figs. 2** and **3**. All the examined coatings have thickness of 300 μm and were sprayed at arc current of 500 A (for sprayed samples at different spraying distances). It is clear from the figure that, the crystallinity of the HA coatings increases as the spraying distance decreases mainly due to the increase of the droplet temperature at the moment of impingement.

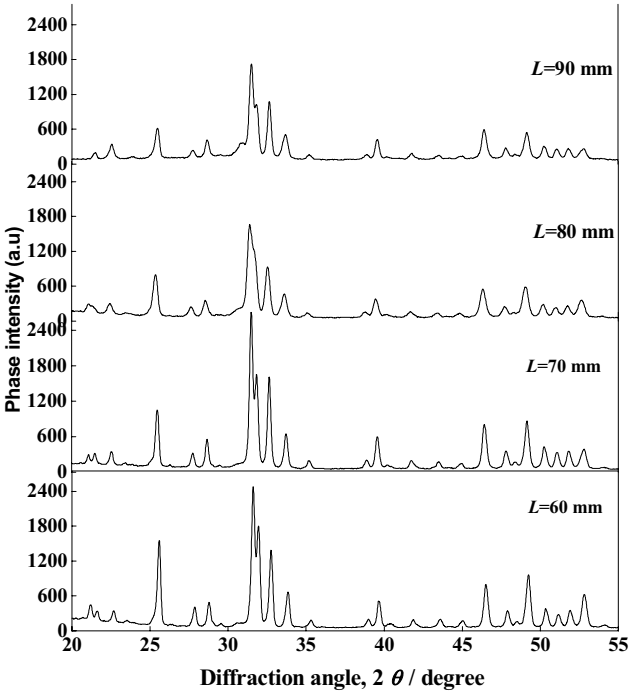

Fig. 2 XRD patterns of HA coatings sprayed at different spraying distances.

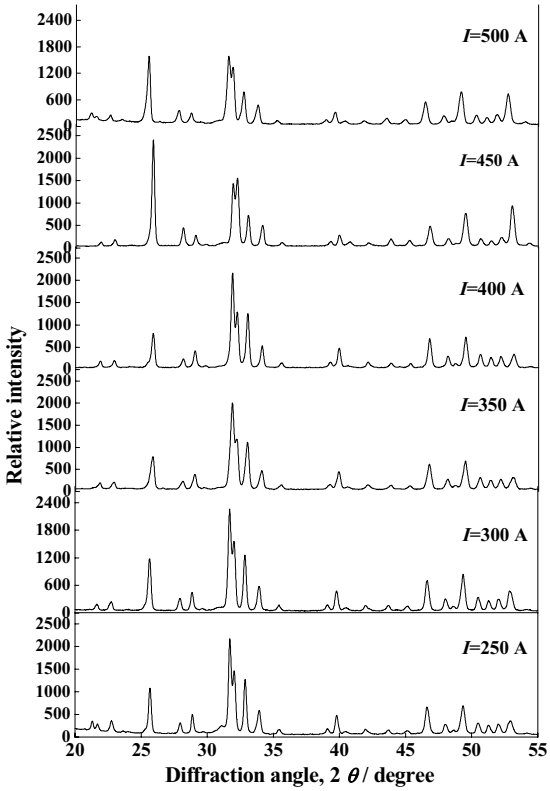

Fig. 3 XRD patterns of HA coatings sprayed at different arc currents.

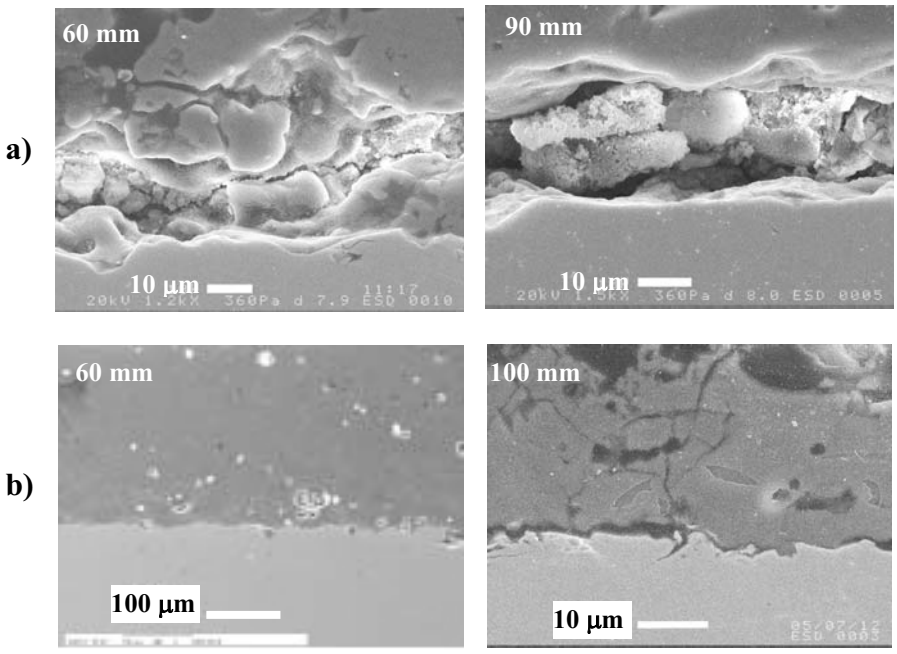

Fig. 4: SEM micrographs of cross-sections of sprayed HA coatings at different spraying distances: a) room temperature and b) 600 K.

At short spray distances the droplets are semi or fully melted (Arc current is 500 A) and as a result the HA phases become more crystalline because the solidification rate gradually decreases as the coating thickness increases.

For samples sprayed at different arc currents, the patterns show that all HA coatings are crystalline with nearly the same phase intensities except those sprayed at 450 and 500 A. As shown in Fig. 3, the intensities of peaks (002), (004, 411) increased for HA coatings sprayed at 450 and 500 A. On the other hand, the intensity of the peak (211) decreased, although it represents almost 100 % (relative intensity) of the peaks for HA coatings sprayed at 250, 300, 350 and 400 A. For coating sprayed at 500 A the intensity of peak (002) decreased compared with that sprayed at 450 A. From the phase structure results, we can conclude that there is a change in phase crystallography (orientation) of HA coatings sprayed at high arc current. This explains the increase of the intensities of (002) and (004,411) peaks as illustrated in the XRD patterns.

3.2 Coatings morphologies

3.2.1 Morphology of HA coatings sprayed at different spray distances

Two set of experiments have been done at two different preheat substrate temperature. One set at room temperature and the other at 600 K. The interface morphologies of the coatings cross-sections of both sets have been investigated by SEM. Figure 4 shows the cross-sections of coated samples at room temperature (**Fig. 4a**) and 600 K (**Fig. 4b**). Samples sprayed at room temperature showed micro-cracks at the interface with the amorphous phase of 5-10 μm thickness. On the other hand, samples sprayed at the preheat substrate temperature of 600K showed no cracks and exhibited good adhesion with the substrate. This experiment illustrates how the substrate temperature greatly affects the interface structure. At room temperature a rapid quenching of flight droplets leads to the formation of an amorphous layer (interface layer) which is separated from the substrate due to the weak adhesion between this layer and substrate. Preheating the substrate decreases the cooling rate of in coming droplets and good wetting occurs between the substrate and the first coating lamella. These enhance the mechanical adhesion and prevent the interface layer from detecting at the interface as well as reduce the residual stress in the HA coatings.

3.2.2 Morphology of HA coatings sprayed at different arc currents

Scanning electron micrographs of HA coatings sprayed at different arc currents are shown in **Fig. 5.** It is clear from Fig. 5 that the coatings sprayed at low arc current (250-400 A) are porous (black spots). However, coatings sprayed at high arc current (450 and 500 A) are dense with low porosity. The presence of pores inside the coatings is related to unmelted HA powders due to the low temperature of the plasma flame at low arc current. At high arc current the flame temperature increases and the heat transfer from the flame to the particles is sufficient to completely melt the powder and as a result dense coatings are formed.

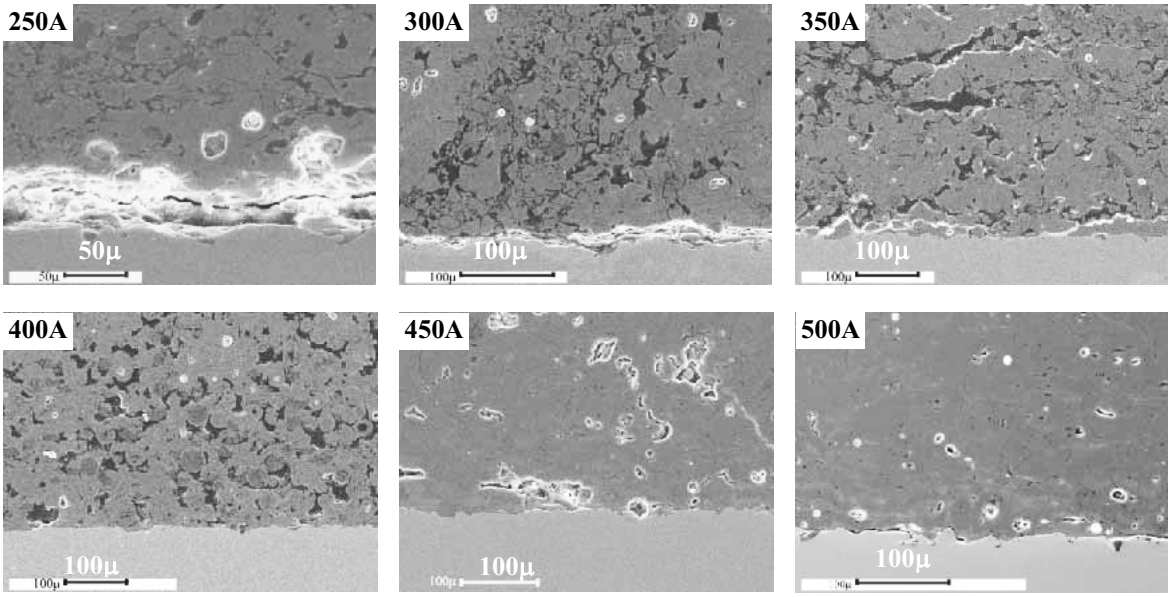

Fig. 5 SEM micrographs of HA coatings sprayed at different arc currents and spraying distance of *L*=60mm.

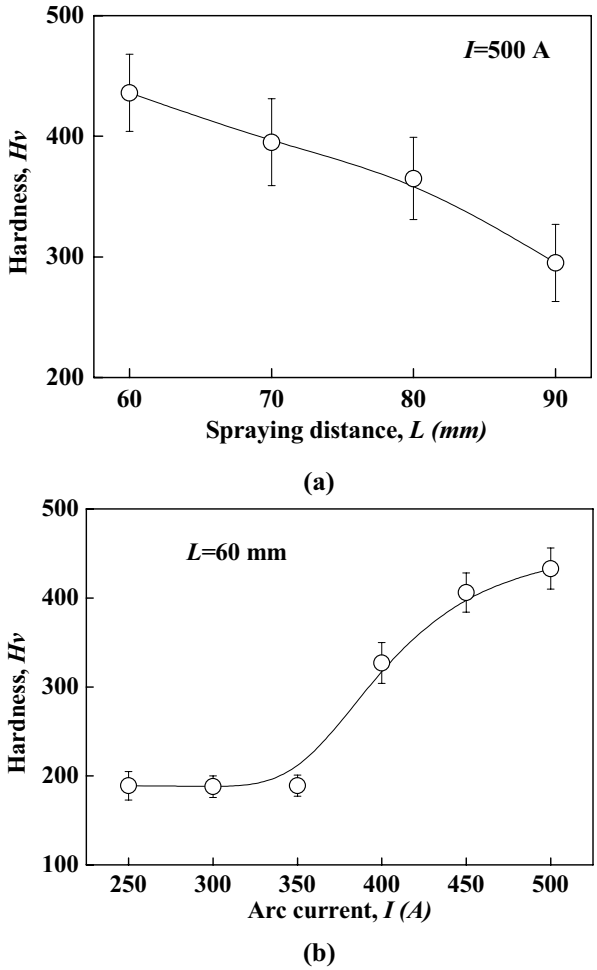

Fig. 6 Hardness measurements of HA coatings at different spray distances and arc currents.

3.3 Hardness

The hardness of HA coatings sprayed at different spraying distances and arc current of I = 500 A and is shown in **Fig. 6 a**. The hardness of HA coatings sprayed at different arc currents and spraying distance of 60 mm is shown in **Fig. 6 b**. The results show that, the hardness of HA coatings increases as the spraying distances decreases and arc current increases, mainly due to the formation of dense coatings with low porosity. Non-melted powders and pores decrease the coating hardness because the cohesion bonding of accumulated particles becomes weak.

4. Conclusions

Hydroxyapatite coatings were plasma sprayed using the gas tunnel type plasma spraying at different spraying distances and arc currents and the following results were obtained:

(1) The Vickers hardness of HA coatings was increased when spraying at short spraying distances and at higher arc currents because of the formation of dense coatings.

(2) The coatings porosity decreased as the arc currents increased because the flight droplets are fully melted and impact together in compact manner to form dense structure coatings.

(2) HA coatings with porous structures were observed at low arc currents, because unmelted powders were found in the coatings.

(3) Cracks appeared at the interface of HA coatings sprayed at room temperature mainly due to the rapid quenching of particles impacting the substrate surface.

Acknowledgment

This work was financially supported by Japan Society for the Promotion of Science (JSPS) Grant-on-Aid (No. 17.05 102).

References

1) R.G.T. Geesink. K. de Groot and C.P.A.T. Klein, *C/in. Orrho. Relat. Res*., Vol 225 (1987) pp 147-170.
2) SD. Cook, K. Thomas, J.F. Kay and M. Jarcho. *Clin. &rho. Relat. Res*., Vol 232 (1988) pp 225-243.
3) A. Ravaglioli and A. Kraejewski. Bioceratnita: Materials, Properties and Applications, Chapman and Hall. London, 1992.
4) B.L. Barthell, T.A. Archuleta and R. Kossowsky. Mater. Res. Ser. Symp. Proc., (1988) pp 709-713.
5) V.W. Raemdonck, P. Ducheyne and D.P. Meester, *J. Am. Ceram. Sot*., Vol 67 (1984) 381--384.
6) K. Yamashita, T. Arashi, K. Kitagaki. S. Yamada, T. Umegaki and K. Ogawa. *J. Am. Ceram. Sot*., Vol 77 (1994) pp 2401-2407.
7) S.J. Ding, C.P. Ju, J.H. Chern Lin, *J. Mater. Sci.: Mater. Med*. Vol 11 (2000) pp 183.
8) C.S. Kim, P. Ducheyne, *Biomaterials* Vol 12 (1991) pp 461.
9) X. Nie, A. Leyland, A. Matthews, *Surf. Coat. Technol.* Vol 125 (2000) pp 407.
10) M. Shirkhanzadeh, *J. Mater. Sci. Lett*. Vol 10 (1991) pp 1415.
11) H.C. Gledhill, I.G. Turner, C. Doyle, *Biomaterials* Vol 20 (1999) pp 315-322.
12) P.L. Silva, J.D. Santos, F.J. Monteiro, J.C Knowles, *Surf. Coat. Technol.* Vol I02 (1998) pp 191-196.
13) R.S. Lima, K.A. Khor, H. Li, P. Cheang , B.R. Marple, *Mater Sci Eng*. A 396 (2005) pp 181–187.
14) S. Dyshlovenko, L. Pawlowski, P. Roussel, D. Murano, A. Le Maguer, *Surf. Coat. Technol*., In Press, Corrected Proof, Available online 17 February 2005
15) Limin Sun, Christopher C. Berndt, Clare P. Grey, *Mater Sci. Eng*. A360 (2003) pp 70-84
16) A. Kobayashi, Y. Arata, and Y. Habara, *J. High Tem. Soc*. Vol 13 (3) (1987) pp 116-124.
17) Y. Arata and A. Kobayashi, *J. Appl. Phys*. 59 (9) (1986) pp 3038-3044.
18) A. Kobayashi, *Weld. International*, Vol 4 (4) (1990) pp 276-282.
19) Y. Arata, A. Kobayashi and Y. Habara, *J. Appl. Phys*. Vol 62 (12) (1987) pp 4884-4889.
20) M. F. Morks**,** Akira Kobayashi**,** International Symposium on Smart Processing Technology, ISMPT 14-15 Nov. 2005, Osaka, Japan